Calculation of giant magnetoresistance in laterally confined multilayers in the current-in-plane geometry

Kingshuk Majumdar, Jian Chen, and Selman Hershfield
Department of Physics and National High Magnetic Field Laboratory, University of Florida, 215 Williamson Hall, Gainesville, Florida 32611
(Received 8 July 1997)

We have studied the giant magnetoresistance (GMR) for laterally confined multilayers, e.g., layers of wires, using the classical Boltzmann equation in the current-in-plane geometry. For spin-independent specularity factors at the sides of the wires we find that the GMR due to bulk and surface scattering decreases with lateral confinement. The length scale at which this occurs is of the order of the film thickness and the mean free paths. The precise prefactor depends on the relative importance of surface and bulk scattering anisotropies. For spin-dependent specularity factors at the sides of the wires the GMR can increase in some cases with decreasing width. The origin of the change in the GMR in both cases can be understood in terms of lateral confinement changing the effective mean free paths within the layers. [S0163-1829(98)06805-2]

I. INTRODUCTION

Electrical transport properties of magnetic multilayers, which are thin alternating layers of ferromagnets (FM's) and paramagnets (PM's), has drawn considerable interest in recent years.[1] A large decrease in the resistivity from antiparallel to parallel alignment of the film magnetizations has been observed experimentally.[2,3] This phenomenon is known as the giant magnetoresistance (GMR). The decrease in the resistivity from antiparallel to parallel alignment arises from spin-dependent scattering.[2] The two sources of spin dependent scattering in these multilayers are bulk scattering and surface scattering. There have been numerous experimental and theoretical studies to understand the physics of the giant magnetoresistance and to use it in applications.[1,4]

There are several theoretical approaches to transport in magnetic multilayers. One approach is to use the phenomenological Fuchs-Sondheimer theory of thin-film resistance.[5,6] This approach is based on the classical Boltzmann equation. Other approaches are based on the linear-response theory[7–9] and the quantum Boltzmann equation.[10] It has been shown that the conductivities obtained from the classical Fuchs-Sondheimer theory are in good agreement with the quantum results obtained via the Kubo formula.[11] Thus it is useful to use the semiclassical approach to understand the physics of the giant magnetoresistance. Furthermore, this method with spin-dependent interface scattering[12] reproduces the qualitative features of the giant magnetoresistance seen in the experiments.[2,3]

With the development of nanotechnology, it is becoming important to understand the effect of lateral confinement on the GMR.[13] In this paper, we address the following questions: (i) Does the GMR increase or decrease with the reduction in width? (ii) If there is an increase or decrease in the GMR what causes it? (iii) What are the relevant length scales in the problem? We use the classical Boltzmann equation to answer the above questions. It is important to note that our calculations only apply to the current-in-plane (CIP) geometry—not the current-perpendicular-to-plane geometry.

The layout of the rest of our paper is as follows. In Sec. II a detailed description of the model and our numerical procedure is given. In Sec. III we present the results of our calculation, and Sec. IV contains the conclusion.

II. THE MODEL

The geometry of our problem is shown in Fig. 1. We compute the current-in-plane conductivity (CIP) for a three-wire structure stacked along the $\hat{y}$ direction. Both the current and the electric field are in the $\hat{z}$ direction. We have two identical ferromagnetic materials (FM) and a paramagnet (PM). For this three-wire geometry we compute the conductivity in the case when the ferromagnet's magnetizations are parallel σ_F, and when they are antiparallel σ_{AF}. The magnetoresistance is defined as the ratio of the change in the conductivity from parallel to antiparallel alignments divided by the parallel conductivity:

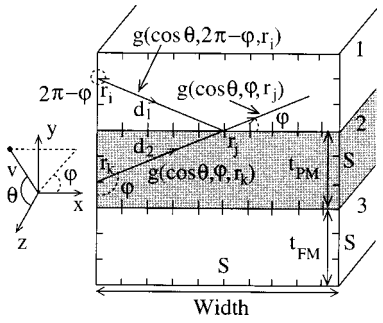

FIG. 1. Schematic diagram of the three-wire structure. Wires 1 and 3 are the ferromagnets of thickness t_{FM}, and wire 2 is a paramagnet of thickness t_{PM}. Current is in plane (CIP) along the $\hat{z}$ direction, and the wires are stacked in the $\hat{y}$ direction. S represents the spin-independent specularity factors at the sides of the ferromagnet, and the paramagnet. To determine the distribution function for outgoing electrons at point $\mathbf{r}_j$, $g(\cos\theta,\phi,\mathbf{r}_j)$, one must consider all possible incoming electrons from points on the edges and interfaces, e.g., points $\mathbf{r}_i$ and $\mathbf{r}_k$. The precise relationship is described in the text [see Eq. (9)].

 © 1998 The American Physical Society

$$\mathrm{GMR}=1-\frac{\sigma_{AF}}{\sigma_F}. \tag{1}$$

To calculate the conductivities for different spin alignments we consider the classical steady-state Boltzmann transport equation:

$$\mathbf{v}\cdot\nabla_{\mathbf{r}}f(\mathbf{v},\mathbf{r})-\frac{e}{m}\mathbf{E}\cdot\nabla_{\mathbf{v}}f(\mathbf{v},\mathbf{r})=\left(\frac{\partial f(\mathbf{v},\mathbf{r})}{\partial t}\right)_{\text{scatt}}, \tag{2}$$

where $f(\mathbf{v},\mathbf{r})$ is the distribution function for electrons of mass m at position $\mathbf{r}$ with velocity $\mathbf{v}$ in presence of the electric field $\mathbf{E}$. Because of the scattering term, Eq. (2) is complicated. For simplicity we consider the case where the scattering term is

$$\left(\frac{\partial f(\mathbf{v},\mathbf{r})}{\partial t}\right)_{\text{scatt}}=-\frac{f(\mathbf{v},\mathbf{r})-\langle f(\mathbf{v},\mathbf{r})\rangle}{\tau}, \tag{3}$$

with $\langle f(\mathbf{v},\mathbf{r})\rangle$ being the spherical average of the distribution function, and τ is the relaxation time. This is the simplest scattering term to represent elastic scattering. To solve Eq. (2) with the right-hand side of Eq. (3), we define $g(\mathbf{v},\mathbf{r})$ to be the deviation of the distribution function from its equilibrium value:

$$f(\mathbf{v},\mathbf{r})=f^{\text{eq}}(|\mathbf{v}|)+g(\mathbf{v},\mathbf{r}). \tag{4}$$

We next make the ansatz that within linear response the spherical average of the distribution function is equal to the equilibrium distribution function, $\langle f(\mathbf{v},\mathbf{r})\rangle=f^{\text{eq}}(|\mathbf{v}|)$, i.e., the spherical average of $g(\mathbf{v},\mathbf{r})$ is zero. This will be checked explicitly later. The linearized Boltzmann equation for a wire labeled by an index n is then given by

$$\mathbf{v}\cdot\nabla_{\mathbf{r}}g_{ns}(\mathbf{v},\mathbf{r})-\frac{e}{m}\mathbf{E}\cdot\nabla_{\mathbf{v}}f^{\text{eq}}_{ns}(|\mathbf{v}|)=-\frac{g_{ns}(\mathbf{v},\mathbf{r})}{\tau_{ns}}, \tag{5}$$

where s denotes the spin of the electrons. When the electric field is zero, Eq. (5) becomes a homogeneous equation with the expected solution being $g_{ns}(\mathbf{v},\mathbf{r})=0$. For nonzero electric field, $g_{ns}(\mathbf{v},\mathbf{r})$ is proportional to $(e\mathbf{E}/m)\nabla_{\mathbf{v}}f^{\text{eq}}_{ns}(|\mathbf{v}|)=e\mathbf{E}\cdot\mathbf{v}\partial f^{\text{eq}}_{ns}(|\mathbf{v}|)/\partial\epsilon_v$. Thus, $g_{ns}(-\mathbf{v},\mathbf{r})=-g_{ns}(\mathbf{v},\mathbf{r})$, irrespective of the boundary conditions, and the ansatz that the spherical average of $g_{ns}(\mathbf{v},\mathbf{r})$ is zero is justified.

The general solution of the above equation[14] is

$$g_{ns}(\mathbf{v},\mathbf{r})=g_{ns}(\mathbf{v},\mathbf{r_B})e^{-|\mathbf{r}-\mathbf{r_B}|/\tau_{ns}|\mathbf{v}|}+e\tau_{ns}\mathbf{E}\cdot\mathbf{v}\left(\frac{\partial f^{\text{eq}}_{ns}}{\partial\epsilon_v}\right)(1-e^{-|\mathbf{r}-\mathbf{r_B}|/\tau_{ns}|\mathbf{v}|}), \tag{6}$$

where $\mathbf{r}_B$ is a point on the boundary or interface. Equation (6) implies that to find the distribution function at position $\mathbf{r}$ with velocity $\mathbf{v}$, we proceed from $\mathbf{r}$ backwards along $\mathbf{v}$ until we reach a point $\mathbf{r}_B$ at the boundary. The distribution function at the boundary, $g_{ns}(\mathbf{v},\mathbf{r_B})$, is determined by the boundary conditions. We recover the usual bulk value if we go far away from the boundary points. Also we can see from Eq. (6) that the electrons lose their momentum as they diffuse into the medium and the characteristic length scale for this is just the mean free path, $\tau_{ns}v_F$, where v_F is the Fermi velocity.

We now examine the boundary conditions. At each interface the electrons undergo either specular or diffuse scattering. For the nth interface, which is between wires n and n $+1$, we define the probability of spin s electrons being diffusively scattered as $(1-S_{ns})$, where S_{ns} is the spin-dependent specularity factor. The probabilities for being specularly reflected and transmitted are $S_{ns}R_{ns}$ and $S_{ns}T_{ns}$, respectively. The sum of R_{ns} and T_{ns} is one. The angular dependence of the surface scattering parameter,[15] the reflection coefficients, and the transmission coefficients[16,17] has been studied, but in our calculation we treat those as angle independent. With these definitions, the boundary conditions at the nth interface can be expressed as

$$g^{\text{out}}_{ns}(\mathbf{v},x,y_n)=S_{ns}T_{ns}g^{\text{in}}_{n-1s}(\mathbf{v},x,y_n)+S_{ns}R_{ns}g^{\text{in}}_{ns}(-\mathbf{v},x,y_n), \tag{7}$$

$$g^{\text{out}}_{n-1s}(-\mathbf{v},x,y_n)=S_{ns}T_{ns}g^{\text{in}}_{ns}(-\mathbf{v},x,y_n)+S_{ns}R_{ns}g^{\text{in}}_{n-1s}(\mathbf{v},x,y_n), \tag{8}$$

where y_n is the position of the interface, and the superscripts out, in correspond to electrons going out from the boundary or coming in to the boundary. Similar equations are satisfied at the sides of the wires except that there is no transmission.

We use an iterative procedure to compute the distribution functions, $g^{\text{out}}_{ns}(\mathbf{v},\mathbf{r_B})$, which are nonuniform along the $\hat{x}$ and $\hat{y}$ directions of the interfaces and edges (see Fig. 1). From Eq. (5), we observe that the $g^{\text{out}}_{ns}(\mathbf{v},\mathbf{r})$'s with different velocities projected along the $\hat{z}$ direction are decoupled. This allows us to discretize the $g^{\text{out}}_{ns}(\mathbf{v},\mathbf{r})$ according to $\cos\theta=v_z/|v|$ and solve each separately. For each $\cos\theta$, $g^{\text{out}}_{ns}(\mathbf{v},\mathbf{r})$ at the edges and the interfaces carry two more indices: an angle ϕ and a position $\mathbf{r}_i$. The $g^{\text{out}}_{ns}(\mathbf{v},\mathbf{r})$'s for different ϕ and $\mathbf{r}_i$ are related via Eq. (6) and the boundary conditions given in Eqs. (7) and (8). To illustrate this we consider the relations between the distribution functions of the outgoing electrons at the first interface in Fig. 1:

$$g^{\text{out}}_{1s}(\cos\theta,\phi,\mathbf{r}_j)=S_{1s}R_{1s}g^{\text{out}}_{1s}(\cos\theta,2\pi-\phi,\mathbf{r}_i)e^{-d_1/\tau_{1s}v_F\sin\theta}+S_{1s}T_{1s}g^{\text{out}}_{2s}(\cos\theta,\phi,\mathbf{r}_k)e^{-d_2/\tau_{2s}v_F\sin\theta}, \tag{9}$$

where d_1, d_2 are the path lengths projected onto the x-y plane from one boundary to another. Initial guesses for $g^{\text{out}}_{ns}(\cos\theta,\phi,\mathbf{r}_i)$ are taken from the nearby $g^{\text{out}}_{ns}[\cos\theta-\delta(\cos\theta),\phi,\mathbf{r}_i]$. The calculations are converged to within 1% with the total number of divisions for $\cos\theta$, $\mathbf{r}_i$, and ϕ chosen as $N_{\cos\theta}=100$, $N_\phi=500$, and $N_i=400$, respectively.

Once the distribution functions at the boundaries are known, by using Eqs. (4) and (6) the distribution function of the electrons with momentum $\mathbf{v}$ at any point $\mathbf{r}$ can be determined. We explicitly check that our ansatz is valid: $\langle g_{ns}(\mathbf{v},\mathbf{r})\rangle=0$. The current density along the direction of the electric field for wire n and spin s is

$$\mathcal{J}_{ns}(\mathbf{r})=-e\left(\frac{m}{h}\right)^3\int v_z g_{ns}(\mathbf{v},\mathbf{r})d^3\mathbf{v}. \tag{10}$$

The conductivity is obtained by averaging the current density over a cross-sectional area, $\mathcal{A}$:

$$\sigma=\frac{1}{E\mathcal{A}}\sum_{n=1}^{3}\sum_{s=\uparrow,\downarrow}\int\mathcal{J}_{ns}(x,y)dxdy. \tag{11}$$

Finally, the giant magnetoresistance is obtained from Eq. (1) using parallel and antiparallel alignments of the magnetizations in Eq. (11).

III. NUMERICAL RESULTS

We begin this section with the different input parameters of our problem. They are the spin-dependent mean free paths in the ferromagnet $L^{\uparrow,\downarrow}$, the mean free path in the paramagnet L^{PM}, the spin-dependent transmission coefficients $T^{\uparrow,\downarrow}$, the specularity factors S, and the thicknesses of the layers t_{FM} and t_{PM}. We choose the mean free paths to be those determined in an experiment on a Co/Cu/Co structure:[18] $L^{\uparrow}=55$ Å, $L^{\downarrow}=10$ Å, and $L^{\mathrm{PM}}=226$ Å. The transmission coefficients are obtained from an average of the transmission coefficients calculated by Stiles:[17] $T^{\uparrow}=0.8$ and $T^{\downarrow}=0.4$. We take the specularity factors at all interfaces and sides to be the same: $S=0.9$. Finally, the thicknesses are chosen to be those of Cu when the Co layers are antiferromagnetically coupled at zero field.[19] For simplicity we take the ferromagnets to have the same thicknesses as the paramagnets: $t_{\mathrm{FM}}=t_{\mathrm{PM}}$.

With the above parameters the giant magnetoresistance is due to both spin anisotropies in the bulk and surface scattering. It is useful to consider the limiting cases when the GMR is due to only bulk scattering anisotropies or only surface scattering anisotropies. To do this, we consider two special cases: (a) when the transmission coefficients are equal: $T^{\uparrow}=T^{\downarrow}=0.6$ and (b) when the bulk mean free paths in the ferromagnet are equal: $L^{\uparrow}=L^{\downarrow}=17$ Å. In the following these are referred to as the (a) bulk scattering case and (b) surface scattering case.

In Fig. 2 we plot the giant magnetoresistance as a function of width for the three cases: (a) GMR due to bulk scattering anisotropies, (b) GMR due to surface scattering anisotropies, and (c) GMR due to both bulk and surface scattering anisotropies. In all cases the giant magnetoresistance decreases as we reduce the width. To understand this decrease with lateral confinement we consider a slab, i.e., a wire with infinite width. Diffusive scattering at the sides of the wire reduces the conductivity and mean free paths of the wire compared to the slab. This reduction in the conductivity in going from a slab to a wire should be comparable to the reduction in going from a bulk system to a slab with a thickness equal to w. The conductivity of such a slab is given by[6]

$$\sigma_{\mathrm{slab}}=\left(\frac{ne^2L}{mv_F}\right)\left\{1-\frac{3L}{2w}(1-S)\times\int_0^1 d(\cos\theta)\cos\theta\sin^2\theta\frac{1-\exp(-w/L|\cos\theta|)}{[1-S\,\exp(-w/L|\cos\theta|)]}\right\},\tag{12}$$

and the bulk conductivity is

$$\sigma_{\mathrm{bulk}}=\left(\frac{ne^2L}{mv_F}\right),\tag{13}$$

where L is the mean free path of the electrons. We obtain an effective mean free path, L_{eff}, by replacing L in Eq. (13) with L_{eff} such that $\sigma_{\mathrm{bulk}}=\sigma_{\mathrm{slab}}$. The effective mean free paths can be used in a multilayer calculation with infinite width wires. The results of such an effective mean-free-path multilayer calculation are plotted as the solid lines in Fig. 2. This approximation is in good agreement with the exact results (symbols), and hence we conclude that the reduction in the GMR is due to a decrease in the effective mean free path within the layers.

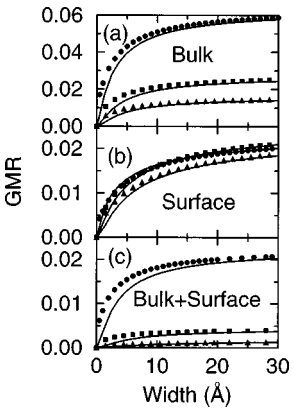

FIG. 2. Giant magnetoresistance of a three-wire structure as a function of width for (a) bulk scattering, (b) surface scattering and (c) both bulk and surface scattering. The symbols refer to different film thicknesses, $t_{\mathrm{PM}}=t_{\mathrm{FM}}=8$ Å (circle), 20 Å (box), and 30 Å (triangle). In all cases the GMR decreases as we laterally confine the multilayers. The origin of this decrease in the GMR can be understood in terms of changing the effective mean free paths in the wires. As the wire width is reduced the effective mean free path within each wire decreases. To make this more quantitative we obtain an effective mean free path for each wire and use these mean free paths in a multilayer calculation (infinite width wire). The results, which are shown as the solid lines, are in good agreement with the exact calculation (symbols). For cases (a) and (c) the mean free paths are chosen for a Co/Cu/Co structure, (Ref. 18) which has $L^{\uparrow}=55$ Å, $L^{\downarrow}=10$ Å, and $L^{\mathrm{PM}}=226$ Å. For case (b), in which only surface scattering contributes to the GMR, we use $L^{\uparrow}=L^{\downarrow}=17$ Å and $L^{\mathrm{PM}}=226$ Å. For cases (b) and (c) the transmission coefficients at the interfaces are taken to be $T^{\uparrow}=0.8$, $T^{\downarrow}=0.4$ (Ref. 17), while for case (a), where the GMR is due only to bulk scattering, we take $T^{\uparrow}=T^{\downarrow}=0.6$. The thicknesses for wire 2 are chosen to be that of Cu when the Co slabs are antiferromagnetically coupled (Ref. 19) and for simplicity we choose the Co layers to have the same thickness as the Cu. In all cases the sides and the interfaces have a specularity factor $S=0.9$.

Although the GMR is reduced in all the cases shown in Fig. 2, the actual GMR vs width curves are different. In particular, there are different length scales at which the GMR is reduced. The width at which the GMR is half its infinite width value, GMR(wire)/GMR(slab) $=1/2$, is defined as the half-width. In Fig. 3 we have rescaled the GMR vs width curves shown in Fig. 2 by GMR(slab) and the half-width. All the points fall close to a single curve. This means that the half-width and the GMR for infinite width wires, GMR(slab), determine the GMR vs width curves. We have also tried the same rescaling with other values of S, which is still the same for all sides and interfaces, and found the same curve.

In Figs. 4(a)–4(c) we have plotted the half-width as a function of the mean free paths in the ferromagnet and the thicknesses. Cases (a)–(c) refer to the same parameters as in Fig. 2. The ratio between the mean free paths in the ferro-

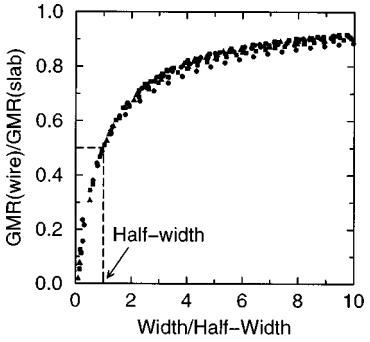

FIG. 3. Rescaled giant magnetoresistance as a function of width. For large width the GMR for a wire approaches that for an ordinary unconfined multilayer, GMR(slab). We define the width at which the GMR is reduced to half of GMR(slab) as the half-width. Rescaling the giant magnetoresistance by GMR(slab) and the width by the half-width, the GMR vs width curves of Fig. 2 fall onto a single curve. The symbols are the same ones used in Figs. 2(a)–2(c).

magnet is fixed to $L^{\uparrow}/L^{\downarrow}=5.5$ in Figs. 4(a) and 4(c), which is the same ratio used in Figs. 2(a) and 2(c). As for Fig. 4(b), the mean free paths are equal in the surface scattering case of Fig. 2(b): $L^{\uparrow}=L^{\downarrow}$. For bulk scattering anisotropies [Fig. 4(a)] the half-width increases almost linearly with both the thickness and the mean free path. On the other hand, for surface scattering anisotropies [Fig. 4(b)] the half-width depends primarily on the thickness of the film and only weakly on the mean free paths in the ferromagnet. When both surface and bulk scattering anisotropies are present [Fig. 4(c)], the dependence of the half-width on the mean free path and thickness can be complicated. In the region where the half-width has a peak in Fig. 4(c), the GMR has a local minimum as a function of the mean free path. The origin of this local minimum comes from the near cancellation of the GMR from the bulk and surface contributions. The location of this minimum depends primarily on the transmission coefficients.

Although we believe the generic behavior is that the GMR will decrease when the multilayers are laterally confined, one can find parameters where the GMR actually increases with lateral confinement. The two ways we have found to do this are (i) have the sides of the wires introduce additional spin dependence in the scattering and (ii) have the sides of the wires selectively decrease the resistivity in the ferromagnet relative to the paramagnet. The idea behind both of these is again that laterally confining the multilayers reduces the effective mean free paths within each layer. By changing the mean free paths by different amounts, one can tune the GMR. As an example, in Fig. 5 we have plotted the GMR vs width for two cases which differ only by the specularity factor at the sides of the FM. For the solid curve the specularity factors are 0.9 for both spin-up and spin-down electrons, while for the dashed curve the specularity factor at the sides for spin-up electrons is 0.9 and for spin-down electrons is 0.5. The GMR actually increases as one decreases the width of the sample because the mean free path for spin-down electrons decreases more rapidly than the mean free path for spin-up electrons. Such spin-dependent specularity factors may occur naturally or be attainable by coating the sides of the multilayer. Allowing spin-dependent specularity factors at nontransmitting interfaces opens up the possibility

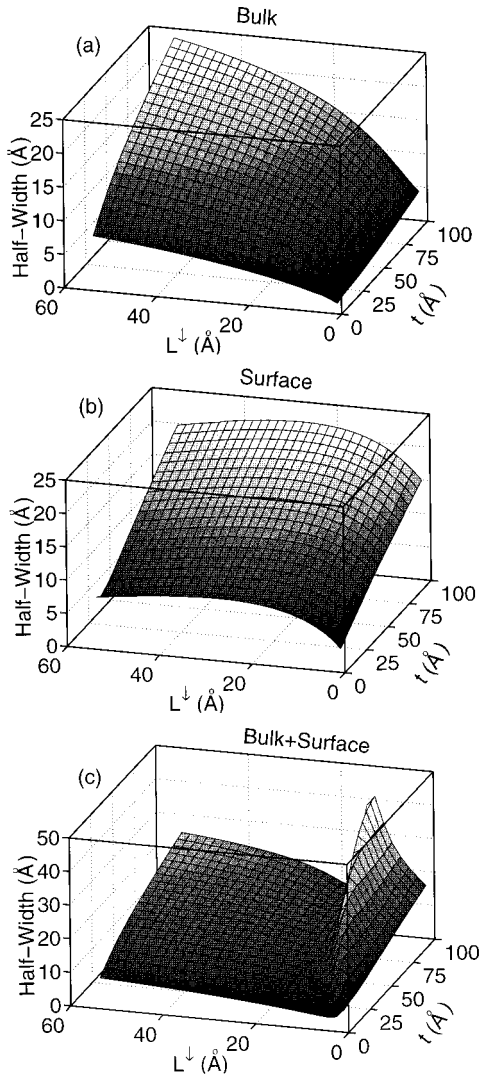

FIG. 4. Half-width as a function of the thickness and mean free path in the ferromagnet ($L^{\downarrow}$) for (a) bulk scattering, (b) surface scattering, and (c) bulk and surface scattering. In (a) and (c) the ferromagnetic spin-up and spin-down mean free paths are kept at a fixed ratio, $L^{\uparrow}/L^{\downarrow}=5.5$, which is the same ratio used in Figs. 2(a) and 2(c). In the surface scattering case of (b) $L^{\uparrow}$ equals $L^{\downarrow}$. The half-width depends both on the thickness and the mean free path for all three cases. In case (a), bulk scattering, the half-width increases roughly linearly with the thickness and the mean free path, while in case (b), surface scattering, the half-width depends primarily on the thickness of the layers. The general case when both bulk and surface scattering are important [case (c)] can lead to complex dependence on the mean free path and film thickness. The feature at small $L^{\downarrow}$ in (c) is associated with the fact that the GMR has a local minimum in this region (see discussion in text). Except for t and $L^{\downarrow}$, which vary, the parameters used in (a), (b), and (c) are the same as in Fig. 2.

that one can create a GMR device without ferromagnetic conductors, but only insulating ferromagnets which change the surface scattering.

IV. CONCLUSION

In this paper we have studied the effect of lateral confinement on the giant magnetoresistance in the CIP geometry.

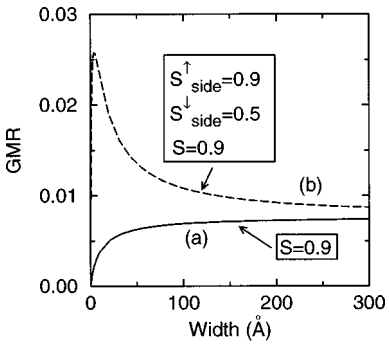

FIG. 5. Giant magnetoresistance as a function of width for (a) spin-independent scattering at the sides and interfaces, (b) spin-dependent scattering at the sides of the ferromagnet. For (a), the GMR decreases with decreasing width (solid line), whereas for (b), the GMR increases with decreasing width (dashed line). The increase of the GMR with reduced width is due to the spin-down mean free path decreasing faster than the spin-up one. For (a), we choose the same parameters as of Fig. 2, except the mean free paths for the spin-up and down electrons in the ferromagnet are 200 and 100 Å, respectively. For (b), we use the same parameters except that the specularity factors for the sides of the ferromagnet are spin dependent: $S^{\uparrow}_{\text{side}}=0.9$ and $S^{\downarrow}_{\text{side}}=0.5$. Note that the GMR eventually goes to zero for small enough widths because the effective mean free path in the paramagnet becomes much smaller than the thickness of the paramagnetic layer.

For spin-independent specularity factors at the sides of the wires, the GMR decreases as one reduces the width of the wires. For this case we found that the GMR vs width curves could be very nearly collapsed onto a single curve by rescaling the GMR by its infinite width value and the width by the half-width. The half-width depends on both the mean free paths and the thickness of the films. In the case of the GMR plays a dominant role in determining the half-width, while in the case of GMR due solely to bulk scattering, the half-width increases roughly linearly with both the mean free paths in the ferromagnetic wires and the thicknesses. The general case when both surface and bulk anisotropies are important can lead to more complex dependences.

The source of the decrease in the GMR in the CIP geometry is a reduction in the effective mean free path in the layers due to scattering off the sides of the wires. We showed this quantitatively by determining an effective mean free path within each wire and substituting it into a multilayer calculation for films (infinite width wires). The results of the approximate solution and the exact solution agree quite well.

For the case of spin-dependent mean free paths we find that there are parameter regimes where the GMR in the CIP geometry can increase as the sample is laterally confined. The origin of the increase is again the changing of the effective mean free path within each layer as one decreases the width. With spin-dependent specularity factors one can change the ratio of the mean free paths for spin-up and spin-down electrons and hence change the GMR. Thus, with appropriately prepared sides of the wires, one may be able to increase or at least stem the decrease in the GMR. In any case the length scale at which the reduction in the GMR takes place is typically quite small, of the order of the mean free paths and the thicknesses of the layers. The effects discussed here will not be important until one goes to very small samples.

ACKNOWLEDGMENTS

This work was supported by DOD/AFOSR Grant No. F49620-96-1-0026 and NSF Grant No. DMR9357474, and the NHMFL. We thank J. Childress and T.S. Choy for helping us in different stages of our work.

[1] Phys. Today **48** (4), 24 (1995).
[2] M. N. Baibich, J. M. Broto, A. Fert, F. Nguyen Van Dau, F. Petroff, P. Etienne, G. Creuzet, A. Friederich, and J. Chazelas, Phys. Rev. Lett. **61**, 2472 (1988); A. Barthélémy, A. Fert, M. N. Baibich, S. Hadjoudj, F. Petroff, P. Etienne, R. Cabanel, S. Lequien, and G. Creuzet, J. Appl. Phys. **67**, 5908 (1990).
[3] G. Binasch, P. Grunberg, F. Saurenbach, and W. Zinn, Phys. Rev. B **39**, 4828 (1989).
[4] R. L. White, IEEE Trans. Magn. **30**, 346 (1994).
[5] K. Fuchs, Proc. Cambridge Philos. Soc. **34**, 100 (1938).
[6] E. H. Sondheimer, Adv. Phys. **1**, 1 (1952).
[7] P. M. Levy in *Solid State Physics: Advances in Research and Applications*, edited by F. Seitz, D. Turnbull, and H. Ehrnereich (Academic, New York, 1994), Vol. 47, p. 367.
[8] H. E. Camblong and P. M. Levy, Phys. Rev. Lett. **69**, 2835 (1992); J. Appl. Phys. **73**, 5333 (1993); H. E. Camblong, Phys. Rev. B **51**, 1855 (1995).
[9] A. Fert and P. Bruno in *Ultrathin Magnetic Structures II*, edited by B. Heinrich and J. A. C. Bland (Springer-Verlag, Berlin, 1994), p. 82; S. S. P. Parkin, *ibid.*, p. 148; A. Fert in *Science and Technology of Nanostructured Magnetic Materials*, edited by G. C. Hadjipanayis and G. A. Prinz (Plenum, London, 1991), p. 221.
[10] P. B. Visscher, Phys. Rev. B **49**, 3907 (1994).
[11] X.-G. Zhang and W. H. Butler, Phys. Rev. B **51**, 10 085 (1995).
[12] R. E. Camley and J. Barnaś, Phys. Rev. Lett. **63**, 664 (1989); J. Barnaś, A. Fuss, R. E. Camley, P. Grunberg, and W. Zinn, Phys. Rev. B **42**, 8110 (1990).
[13] Y. D. Park, J. A. Caballero, A. Cabbibo, J. R. Childress, H. D. Hudspeth, T. J. Schultz, and F. Sharifi, J. Appl. Phys. **81**, 4717 (1997).
[14] R. G. Chambers, Proc. R. Soc. London, Ser. A **202**, 378 (1950).
[15] R. Lenk and A. Knábchen, J. Phys.: Condens. Matter **5**, 6563 (1993).
[16] R. Q. Hood and L. M. Falicov, Phys. Rev. B **46**, 8287 (1992).
[17] M. D. Stiles, J. Appl. Phys. **79**, 5805 (1996).
[18] Bruce A. Gurney, Virgil S. Speriosu, Jean-Pierre Nozieres, Harry Lefakis, Dennis R. Wilhoit, and Omar U. Need, Phys. Rev. Lett. **71**, 4023 (1993).
[19] S. S. P. Parkin, R. Bhadra, and K. P. Roche, Phys. Rev. Lett. **66**, 2152 (1991).